Journal of Structural Biology xxx (2015) xxx–xxx

Contents lists available at ScienceDirect

Journal of Structural Biology

journal homepage: www.elsevier.com/locate/yjsbi

Computer-aided design of aptamers for cytochrome p450 ☆

Dmitrii S. Shcherbinin [a,*], Oksana V. Gnedenko [a], Svetlana A. Khmeleva [a], Sergey A. Usanov [b], Andrei A. Gilep [b], Aliaksei V. Yantsevich [b], Tatsiana V. Shkel [b], Ivan V. Yushkevich [b], Sergey P. Radko [a], Alexis S. Ivanov [a], Alexander V. Veselovsky [a], Alexander I. Archakov [a]

[a] Institute of Biomedical Chemistry RAMS, Pogodinskaya str., 10, Moscow 119121, Russia
[b] Institute of Bioorganic Chemistry of the National Academy of Sciences of Belarus, Kuprevich str., 5/2, Minsk 220141, Belarus

ARTICLE INFO

Article history:
Received 6 April 2015
Received in revised form 25 June 2015
Accepted 9 July 2015
Available online xxxx

Keywords:
Aptamer
Cytochrome P450 51A1
Molecular dynamics
Molecular docking
Rational design
Bioinformatics
SELEX

ABSTRACT

Aptamers are short single-stranded DNA or RNA oligonucleotides that can bind to their targets with high affinity and specificity. Usually, they are experimentally selected using the SELEX method. Here, we describe an approach toward the *in silico* selection of aptamers for proteins. This approach involves three steps: finding a potential binding site, designing the recognition and structural parts of the aptamers and evaluating the experimental affinity. Using this approach, a set of 15-mer aptamers for cytochrome P450 51A1 was designed using docking and molecular dynamics simulation. An experimental evaluation of the synthesized aptamers using SPR biosensor showed that these aptamers interact with cytochrome P450 51A1 with K_d values in the range of 10^{-6}–10^{-7} M.

1. Introduction

Aptamers are short single-stranded DNA or RNA oligonucleotides with stable spatial structures that are capable of binding to their targets with high affinity and specificity (Mayer, 2009). During the last two decades, aptamers have been generated against various targets including small molecules, proteins, co-factors, cell surfaces, whole organisms, and inorganic materials (Balogh et al., 2010; Sefah et al., 2010). These oligonucleotides have several technological advantages over traditional affinity reagents such as antibodies. Aptamers can be selected with high affinity and specificity often comparable to those of antibodies. The selection method is universal and can be adapted to different classes of targets, including toxic compounds. Aptamers do not elicit immunogenic responses and have half-lives that can range from very short to very long, enabling their use for both acute and chronic diseases (Keefe and Schaub, 2008). After development, aptamers are chemically synthesized with high accuracy and reproducibility; they can be chemically modified to enhance their biochemical stability and affinity. Moreover, they can be easily regenerated after denaturation. The unique properties of aptamers result in significant interest in their application in various areas. Thus, aptamers are important novel affinity reagents used in biotechnology (Deng et al., 2001; German et al., 1998; Connor and McGown, 2006; Davis et al., 1998; Tombelli et al., 2005; Ferreira et al., 2008). In addition, aptamers can compete with antibodies as therapeutic agents (Ulrich et al., 2006). The first approved aptamer with therapeutic function is the VEGF aptamer (VEGF, vascular endothelial grow factor); this drug treats the choroidal neovascularization associated with age-related macular degeneration (Ng et al., 2006).

Aptamers are selected *in vitro* from the large libraries of randomized sequences using the SELEX (Systematic Evolution of Ligands by EXponential enrichment) method, which involves multiple cycles of selection and amplification (Stoltenburg et al., 2007). The process of selecting aptamers with high affinity and specificity is time consuming without any guarantee of success. In addition, the aptamer selection process is often compromised by the unspecific binding of the oligonucleotides.

Abbreviations: VEGF, vascular endothelial growth factor; SELEX, Systematic Evolution of Ligands by EXponential enrichment; CYP51, cytochrome p450 51A1, lanosterol 14α-demethylase; MD, molecular dynamics; PME, particle mesh Ewald; MM–PBSA, Molecular Mechanics Poisson–Boltzmann/Surface Area; NMA, normal mode analysis; SASA, solvent-accessible-surface area; RMSD, root-mean-square deviation.

☆ This work was supported by Russian Foundation of Basic Research [Grant No. 13-04-40109-N].

* Corresponding author at: Lab. Structural Bioinformatics, Institute of Biomedical Chemistry RAMS, Pogodinskaya str., 10, Moscow 119121, Russia.
E-mail address: amid.dima@gmail.com (D.S. Shcherbinin).

http://dx.doi.org/10.1016/j.jsb.2015.07.003
1047-8477/

Methods of bioinformatics and rational drug design can be used to optimize aptamer selection for a protein target. Two strategies for rational aptamer design can be proposed. The first is based on generation of a virtual library of sequences, modeling of their 3D-structures and selection of perspective aptamers through docking. This approach has already been realized for the selection of RNA-aptamers (Chushak and Stone, 2009). The problems of this approach include the time-consuming generation of realistic spatial structures and docking of a large pool of aptamers. The second approach is based on the assumption that the aptamer structure can be divided into two parts. The first part interacts directly with the target and participates in target recognition, contributing a significant part of the binding free energy for the aptamer–protein complex; this behavior is similar to the hot spots observed in protein–protein interactions (Ma et al., 2001; Sanchez et al., 2010; Veselovsky and Archakov, 2007). The second part of the aptamer maintains the spatial conformation of the recognition part providing optimal interactions with the target. Consequently, this approach toward aptamer design involves two steps. The first step is the computer-aided design of short sequences that interact with the target and contribute significantly to the binding free energy of the protein–aptamer complex. The second step is the construction of the structural part of the aptamer and the fusion of the both selected parts. This approach is similar to the Fragment-Based Drug Design method that based on selection (experimental or *in silico*) of small compounds able to interact with the target protein and linkage them in one molecule (Kumar et al., 2012; Joseph-McCarthy et al., 2014). Also short peptides or oligonucleotides frequently have been used instead of whole proteins or DNA/RNA molecules in protein–protein or protein–nuclear acids interactions studies (Veselovsky et al., 2007; Dey et al., 2012).

In this paper we show the applicability of the proposed *in silico* approach for targeted aptamer development, which involves the separate design of its parts. This approach was used to design aptamers for human cytochrome P450 51A1. Cytochrome P450 51A1 (lanosterol 14α-demethylase, CYP51) is a crucial enzyme in the sterol biosynthesis pathway (sa Debeljak et al., 2003; Lepesheva and Waterman, 2004) that has been targeted by antifungal drugs (Waterman and Lepesheva, 2005; Gnedenko et al., 2013). The spatial structure of human CYP51 is known (Strushkevich et al., 2010); this structure is promising for *in silico* studies of its enzymatic properties and its affinity toward different compounds (Mukha et al., 2011). The discovered aptamer for CYP51 consists of the recognition (sequence of three nucleotides) and structural (in our case we used double helix) parts. Therefore, the aptamer structure is a 15-mer hairpin loop. The experimental evaluation of the set of synthesized aptamers has shown that these aptamers interact with the target protein with K_d values in the range of $10^{-6}10^{-7}$ M.

2. Materials and method

The spatial structure of human cytochrome P450 51A1 was obtained from the RCSB Protein Data Bank (4JUV). The protein structure was prepared by removing water molecules and optimizing the structure through a short MD simulation (4 ns).

The library of all 64 possible trinucleotides was designed using Sybyl 8.1 software. These structures were minimized using a Tripos force field with Gasteiger–Huckel atomic partial charges.

2.1. Docking

Trinucleotides were docked to CYP51A1 using the DOCK 6.5 program (Lang et al., 2009). The solvent-accessible surface of the target for docking was built based on the Connolly algorithm with a probe radius of 1.4 Å. The electrostatic and van der Waals potential fields generated over the target was calculated using a grid (spacing 0.3 Å); the non-bonded distance cutoff was 12 Å; the parameters for the van der Waals interactions were used from the dw_AMBER_parm99.defn set. The compounds were docked using a grid-based energy scoring option for minimization after their initial placement; the best docking pose was selected based on a scoring function from DOCK 6.5. The poses and conformations of trinucleotides were analyzed using the Sybyl 8.1 software suite.

2.2. Molecular dynamics (MD) and binding energy calculation

The MD simulations were accomplished using the *sander* program from the AMBER 9.0 package (Case et al., 2006). The simulations were performed using periodic boundary conditions and explicit solvation. *XYZ* dimensions of the simulation boxes were approximately 95 × 81 × 92 angstroms. All boxes were filled with a water TIP3P model (~16,000 molecules) and neutralized with Na^+ ions. The ff99-SB force field was used for proteins and the parmbsc0 was used for nucleic acids. Before the MD simulations, all of the complexes were relaxed using a minimization procedure (5000 cycles of steepest descent) followed by gradual heating to 300 K over 50 ps in the NVT ensemble. The system was equilibrated with a target temperature of 300 K and a target pressure of 1 atm over 100 ps. The production simulation ran for 10 ns with a 2 fs step. A particle mesh Ewald (PME) was employed to treat the long-range electrostatic interactions. The cut-off for the non-bonded interactions was 8 Å. The temperature was maintained using Langevin dynamics with a friction coefficient of 2 ps^{-1}, and the pressure was controlled with a Berendsen barostat. A SHAKE procedure was employed to constrain all bonds involving hydrogen atoms, and the integration time step was 2.0 fs.

MD trajectories were processed and analyzed using the AMBER program tool ptraj, the VMD software (Humphrey et al., 1996) and Qtiplot.

All simulations were performed on a local cluster using 32 cores for each simulation.

2.3. Binding energy calculation

The free binding energies for the aptamers–cytochrome P450 complexes were calculated using a Molecular Mechanics Poisso n–Boltzmann/Surface Area method (MM–PBSA) and Normal Mode Analysis (NMA) using the *mmpbsa* and *nmode* programs implemented in Amber9.

The MM–PBSA binding energy consists of two parts: the gas-phase interaction energy between the protein and ligands and the solvation free energy. The gas-phase interaction energy between the protein and ligands is the sum of the electrostatic and van der Waals interaction energies. The solvation free energy is the sum of polar and nonpolar parts. The value of the exterior dielectric constant was set to 80, and the solute dielectric constant was set to 1.0. The nonpolar contribution was determined based on the solvent-accessible-surface area (SASA). The NMA was performed to calculate the conformational entropy change after ligand binding. The corresponding ligand and receptor were extracted from the aptamer–protein complex and each of the structures was fully minimized using 10,000 steps until the root-mean-square of the elements of the gradient vector was less than 0.0001 kcal mol^{-1} E^{-1}. To reduce the computational demand, 10 snapshots were taken from 5 to 7 ns of MD simulations with 200-ps steps. The final values for the free binding energies of aptamer–cytochrome P450 complexes were calculated as the sum of the MM–PBSA and NMA, which were obtained from the average over the snapshots.

Please cite this article in press as: Shcherbinin, D.S., et al. Computer-aided design of aptamers for cytochrome p450. J. Struct. Biol. (2015), http://dx.doi.org/10.1016/j.jsb.2015.07.003

3. Experiment

3.1. Aptamer synthesis

5′-Biotin-labeled oligonucleotides were synthesized on a DNA-synthesizer ASM-800 (Biosset, Novosibirsk, Russia) according to the manufacturer's instruction. The synthesized oligonucleotides were purified using reverse-phase chromatography over Poly-Pak cartridges from Glen Research (Sterling, VA, USA). Thr reagents used in the oligonucleotide synthesis and purification were from Acros Organics (Geel, Belgium) except for the phosphoramidites and ethylthiotetrazole, which were obtained from Glen Research. The biotin was conjugated to the 5′-terminus of the oligonucleotides via a hexaethyleneglycol spacer during the chemical synthesis employing 5′-biotin and spacer 18 phosphoramidites (Glen Research).

3.2. Binding measurements

The HBS-P buffer (10 mM HEPES, pH 7.4, 150 mM NaCl, 0.05% Surfactant P20) was obtained from GE Healthcare (USA). The other reagents of the analytical-grade were obtained from Sigma–Aldrich.

Highly purified recombinant human CYP51A1, human CYP3A4 and cytochrome b_5 type A were expressed in bacteria and purified according to (Strushkevich et al., 2010; Guryev et al., 2001). NADPH-cytochrome P450 reductase was kindly provided by Prof. L.M. Podust (Ivanov et al., 2010). Bovine serum albumin and thrombin from human plasma were obtained from Sigma–Aldrich.

The real-time measurements of the protein interactions with the DNA-oligonucleotides were performed using the SPR biosensor Biacore T200 system (GE Healthcare, USA). The 5′-biotinylated oligonucleotides were immobilized on the surface of streptavidin-coated sensor chip SA (GE Healthcare, USA) at the flow rate of 10 μl/min for 2 min in the HBS-P buffer. Before immobilization, the oligonucleotides were diluted in HBS-P buffer to 10 μg/ml, incubated at 95 °C for 5 min and cooled on ice. Approximately 1000 RU of the biotinylated oligonucleotide was immobilized in one flow cell.

The DNA–protein interactions were monitored by injecting protein diluted to various concentrations (10 nM–1 μM) in 25 mM Na–phosphate buffer (pH 7.2) at 5 μl/min for 5 min. The measurements were performed at 20 °C. The chip was regenerated after each measurement by washing with 0.05% SDS solution for 0.5 min at 50 μl/min.

The interactions were estimated by subtracting the response in a "reference" flow cell from the response in a cell with immobilized oligonucleotides. A blank flow cell was used as the "reference" cell.

3.3. Data processing

The sensograms were analyzed using the BIAevaluation v.4.1 software (GE Healthcare, USA). The equilibrium dissociation constants (K_D) for the complexes of CYP51 with the oligonucleotides were calculated using a nonlinear regression (present in the BIAevaluation v.4.1 software) based on the dependence of the equilibrium biosensor signal on concentration of CYP51:

$$R_{eq}/R_{max} = C/(K_D + C),$$

where R_{max} is the maximal response; C is the concentration of a protein; R_{eq} is the equilibrium response at a given protein concentration.

4. Results

The proposed approach requires the preliminary selection of a potential aptamer binding site. A visual inspection of the CYP51A1 structures showed that there are at least two potential sites for aptamer binding. The negatively charged nucleic acids sequences should bind to the protein surface regions enriched with positively charged amino acid residues. The first potential site is located on the proximal side (relative to the heme co-factor) of the CYP51A1 and the lysine and arginine residues located on the F′ and G-helixes. The second site is located on the opposite axial side of the protein. Initially, the docking of the library containing all possible trinucleotides on the entire surface of the protein was performed to select the most probable aptamer binding sites. Consequently, three possible aptamer binding sites on the CYP51A1 surface were detected (Fig. 1A). The main binding site accommodated approximately 80% of the docked poses located on the axial side of CYP51A1 around Arg448 (the second binding site located by the preliminary structure inspection). The second site was located near the K and K′ helixes and the 1–4β strands (~15% of the docking poses); a minor binding site was predicted by a visual inspection of the protein structures. The docking of the representative set of tetranucleotides showed a similar result (data not shown), but was more time-consuming, so further docking experiments were performed using trinucleotides.

The next docking, focused on the main nucleotide binding site, generated 570 different docking poses for the trinucleotide library. The best value for the Dock6.5 scoring function was found for the GGG oligonucleotide (−113.6 kcal/mol). Analysis of the docking poses showed that the binding site may be subdivided into three regions surrounding Arg448, which can accommodate nucleotides (Fig. 1B). The first region was formed by Tyr426, Ala432, Lys436, Phe437, Val440 and Ala444; the second was formed by Leu163, Asn164, Ile165, Phe168, Tyr354 and Val457; the third was formed by Lys160, Gly445, Arg446, Arg448, Cys449 and Ile450. The distribution of different nucleotides through these regions is shown in

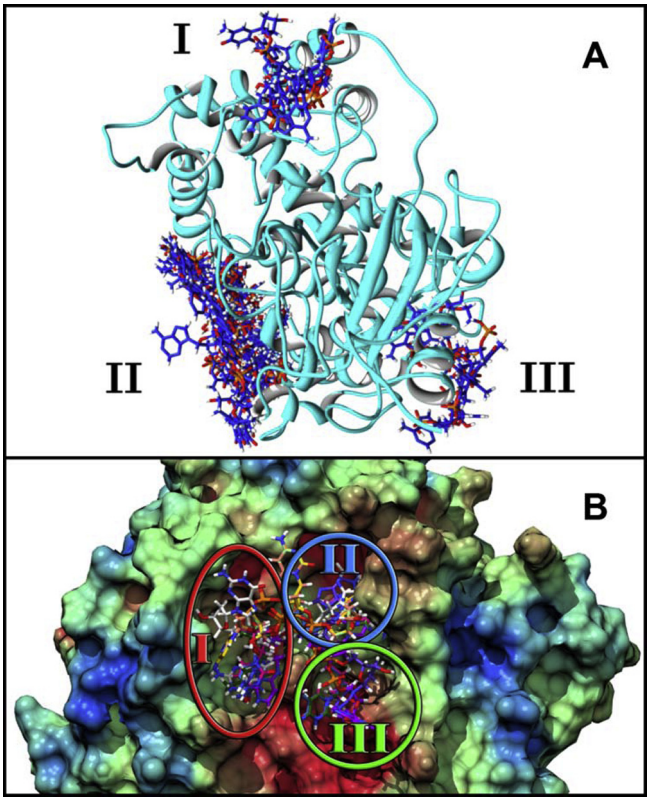

Fig. 1. Distribution of trinucleotides on the surface of cytochrome P450 51A1 obtained by docking. (A) Three potential binding sites on the surface of cytochrome P450 51A1. (B) Distribution of nucleotides in the second binding site.

Table 1. Clearly, the distribution of the nucleotides is not random. Region I prefers to accommodate cytosine, region II prefers guanidine and region III prefers thymine. The second region of the nucleotide-binding site was the most selective. Nevertheless, no docking poses for the CGT trinucleotide were found.

To estimate the ability of nucleotides to bind to cytochrome P450 51A1, we selected seven trinucleotides. Four trinucleotides with the best Dock scoring function values (GGG, TGC, GGT and AGG) and two trinucleotides (CAT and ACA) with low Dock scores were selected. The trinucleotide CGT (the best trinucleotide according to the statistical distribution, Table 1) was also designed and used in the further analysis. The Dock score values for these trinucleotides are shown in Table 2.

The molecular dynamics of cytochrome P450 complexes with all selected trinucleotides was performed to optimize the structure of the complexes; afterward, the binding energies of the trinucleotides–protein complexes were estimated.

The root-mean-square deviation (RMSD) values for the heavy atoms of the cytochrome P450 in the complexes with trinucleotides are shown in Fig. 2A. The amino acid residues deviated rapidly from the initial structures within 2 ns of the MD simulation due to optimization of interactions within the protein structure, as well as with water. The RMSD was stabilized between 1.6 and 2.6 Å. Therefore, the structures of the proteins were well relaxed and stable over the time scale of the simulation.

Table 1
Distribution of nucleotides in the regions of second aptamer-binding site.

	dA	dC	dG	dT
Region I	35	**100**	82	59
Region II	49	54	**179**	40
Region III	143	117	46	**178**

Table 2
Values of Dock score, calculated binding free energies using MM–PBSA and experimental binding affinity (K_d, μM, ΔG, kcal/mol) of seven selected trinucleotides.

Trinucleotide	Dock score (kcal/mol)	ΔG (calculated) (kcal/mol)	K_d (μM)	ΔG (experiment) (kcal/mol)
CAT	−100.00	−5.18	0.6 ± 0.3	−8.54
ACA	−94.80	17.60	1.3 ± 0.3	−8.07
TGC	−109.90	−11.64	0.5 ± 0.2	−8.65
GGT	−105.46	−4.92	0.4 ± 0.1	−8.78
CGT	No data	−19.88	0.28 ± 0.08	−9.37
AGG	−106.60	−18.12	0.15 ± 0.03	−9.41
GGG	−113.60	−18.13	0.14 ± 0.04	−8.54

The RMSD values from the docked poses for the most of the trinucleotides rapidly increased at the beginning of each simulation and had smaller fluctuations after achieving a plateau (Fig. 2B). However the ACA trinucleotide showed complex behavior during the MD simulation. The RMSD dramatically increased within 3 ns before declining to values typical of other trinucleotides, indicating a reorganization in the simulated complex. Therefore, the majority of complexes had the optimal conformation.

To estimate the affinity of the selected trinucleotides, their binding energies to the protein were calculated using an MM–PBSA and NMA methods. The calculations were performed for all complexes from 5 to 7 ns when the structures of the complexes were already equilibrated. The free binding energies were calculated as a sum of the gas-phase energies (including Coulombic interaction energy, the energy of van der Waals interaction determined by a Lennard–Jones potential, and the internal energy), the solvation free energies (including a non-polar portion and an electrostatic portion obtained from the PB calculations) and the entropic terms resulting from the translational, rotational, and vibrational contributions (by NMA method). The binding free energies were obtained as averaged values. These values are given in Table 2, and the lists of the components of the molecular mechanics and solvation energies are given in Supplementary Table 1. The dock scores and binding energies calculated using the MM–PBSA method were correlated with a value of R^2 equal to 0.75. The positive value for the binding energy was obtained for the ACA trinucleotide; its position within the binding site changed during the molecular dynamics (Fig. 2B). The MM–PBSA method predicted the tightest binding for the trinucleotide CGT selected based on the favorable statistical distribution (Table 1) for the nucleotides in three subsites of the binding site during the docking experiments. Therefore, the molecular dynamics and the estimated binding energy of selected trinucleotides suggest that the most of the trinucleotides can interact with the selected binding site on the surface of cytochrome P450 51A1.

The next step was to design of the rigid part of the aptamers, which is used to fix the "binding" conformation of the predicted recognition part. According to the docking results and molecular dynamics, all trinucleotides in the binding site had U-like structures around Arg 448, and the distance between their 5′- and 3′-ends ranged from 15.5 to 16 Å. This distance coincided well with the distance between the 5′- and 3′-ends in hairpin structures of the double helix DNA (based on known 3D-structures of DNA hairpins, this distance varies from 15 to 17.5 Å). Therefore, the rigid part of the designed aptamer might be a double helix that, when fused with the binding part of the aptamer (trinucleotides), would form a DNA hairpin structure. Analysis of the surface of cytochrome P450 51A1 and the electrostatic potential distribution around the selected nucleotide-binding site showed that the

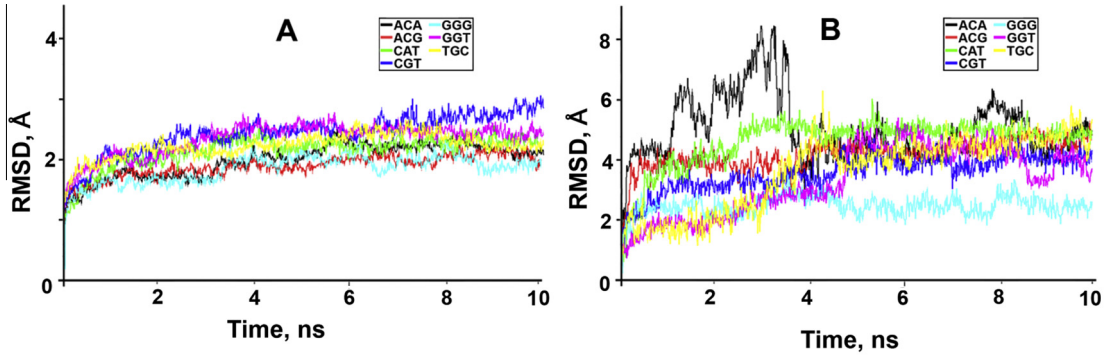

Fig. 2. Root Mean Square Deviation during molecular dynamics simulation of protein–trinucleotide complexes. (A) RMSD values of cytochrome P450 51A1 amino acid residues. (B) RMSD values of nucleotides during MD.

Please cite this article in press as: Shcherbinin, D.S., et al. Computer-aided design of aptamers for cytochrome p450. J. Struct. Biol. (2015), http://dx.doi.org/10.1016/j.jsb.2015.07.003

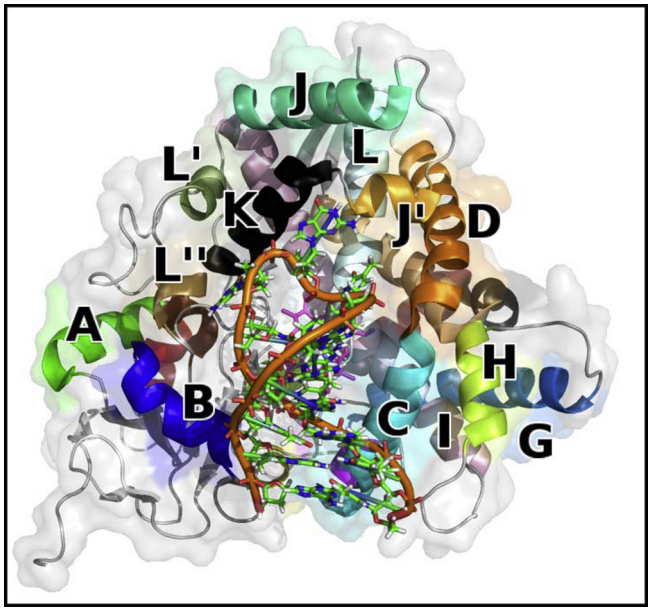

Fig. 3. The structure of the designed 15-mer aptamer bonded to cytochrome P450 51A1.

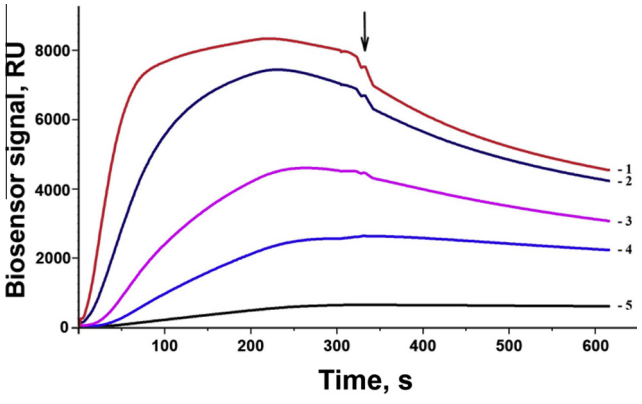

Fig. 4. Sensograms of interaction of aptamers with cytochrome P450 51A1. Arrow shows the start of washing. Concentration of aptamers: 1 – 1 μM, 2 – 500 nM, 3 – 200 nM, 4 – 100 nM, 5 – 50 nM.

elongation of the trinucleotides would not hamper binding to the protein.

To avoid the erroneous folding of aptamers, elongation of the trinucleotides when forming the hairpin-like structure was accomplished using a TTAATT sequence at the 5′-end and its complement at the 3′-end. Therefore, the full sequence of the aptamers for cytochrome P450 51A1 was TTAATTXXXAATTAA, where a double helix forms the rigid (structural) part (TTAATT and AATTAA) and the selected trinucleotides (marked as XXX) define the recognition part of the aptamers. A model of the 3D-structure for a 15-mer aptamer in complex with cytochrome P450 51A1 is shown in Fig. 3. To check the ability of designed aptamers to interact with selected binding site of cytochrome P450 51A1 the initial structure of the aptamer TTAATTCGTAATTAA and five its conformations obtained during 10 ns molecular dynamics were docked to the binding site. During docking search receptor's amino acids and structural part of aptamer were rigid. Only nucleotides of the recognition part of aptamer were flexible. All structures were successfully docked on the surface of selected site with good overlapping with position of initial designed complex. The best conformations are shown in Supplementary Fig. 1S.

Two hairpin-like aptamers using CGT and GGG for recognition were designed; the stability of their complexes with cytochrome P450 51A1 was analyzed using a molecular dynamics simulation. Both complexes of the aptamers with the protein were stable over the whole trajectory of the simulation; therefore, elongation of the aptamers does not disrupt the interaction of the trinucleotide with the target.

Therefore, molecular modeling experiments predicted that several 15-mer hairpin-like oligonucleotides can interact with cytochrome P450 51A1. To test this prediction experimentally, seven selected aptamers were synthesized (Table 2); their binding to cytochrome P450 51A1 was measured using optical biosensor.

The aptamers were immobilized on the surface of an optical chip in the flow cell and cytochrome P450 molecules were floated over the immobilized oligonucleotides. This experimental scheme was chosen to avoid the electrostatic repulsion between the negatively charged aptamers and the carboxylated dextran molecules, as would occur if the protein was immobilized on the chip. All aptamers could interact with cytochrome P450 51A1 (Table 2). The typical sensograms for the aptamer–cytochrome interaction are shown in Fig. 4. The K_d values for the cytochrome P450-aptamer complexes ranged from 1.4×10^{-7} to 1.3×10^{-6} M and decreased in the following order: ACA → CAT → TGC → GGT → CGT → AGG → GGG (only the central parts of the aptamers are listed). This order is similar to that for the trinucleotide sequences obtained during the *in*

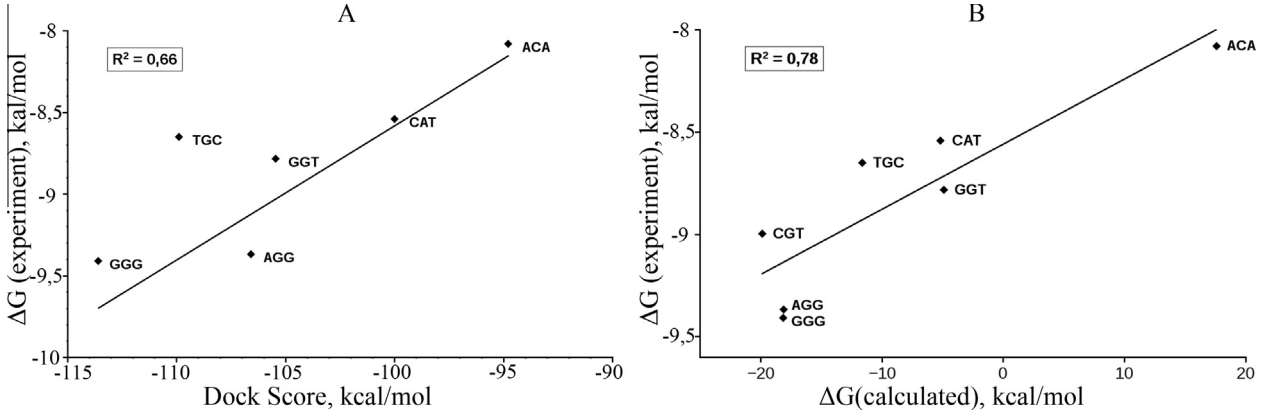

Fig. 5. Comparison between the calculated binding affinity and the experimental ΔG values. (A) Correlation between Dock score and experimental ΔG values; (B) correlation between free binding energy calculated by MM–PBSA method and experimental ΔG values.

Please cite this article in press as: Shcherbinin, D.S., et al. Computer-aided design of aptamers for cytochrome p450. J. Struct. Biol. (2015), http://dx.doi.org/10.1016/j.jsb.2015.07.003

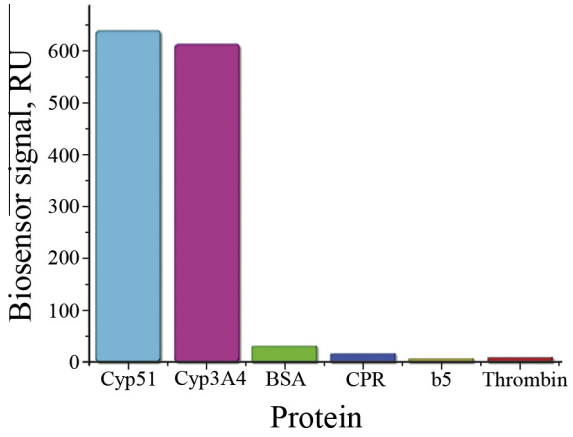

Fig. 6. Selectivity of designed aptamers.

silico experiments used to estimate the aptamers affinities. The correlations (R^2) for the experimental values of K_d values with the Dock scores and the free energies calculated using the MM–PBSA method were 0.66 and 0.78, correspondingly (Fig. 5).

To test the selectivity of the designed aptamers, we have also investigated the binding of five individual proteins (cytochrome P450 3A4, bovine serum albumin, cytochrome b_5 type A, thrombin and NADPH-cytochrome P450 reductase) to the aptamer immobilized on the chip (Fig. 6). The results of these binding experiments clearly indicate that most of the tested proteins did not bind to the aptamers. The exception was cytochrome P450 3A4; its binding affinity was similar to that of cytochrome P450 51A1. Therefore, the designed aptamers are selective for cytochromes P450 but cannot discriminate between members of the cytochrome P450 superfamily.

5. Discussion

Aptamers are a perspective class of compounds used as affinity reagents or drugs (Kanwar et al., 2011; Ni et al., 2011; Citartan et al., 2012). Currently, aptamers are selected using experimental SELEX methods (Stoltenburg et al., 2007); aptamer discovery depends on luck and may be high time consuming and expensive. One of the rational approaches toward aptamer design involves using molecular modeling methods that have proved their effectiveness for discovering small compounds for different targets, including proteins and nucleic acids (Dailey et al., 2009; Barcellos et al., 2008; Ma et al., 2011).

Herein, we have described a new approach toward *in silico* aptamer design. In this approach the aptamers consist of two parts: the recognition and structural parts. The first part is responsible for the interaction with the target and the binding affinity, while the second part preserves the optimal spatial structure of the recognition part.

The developed approach toward aptamer design includes several steps. The first step involves a search for a potential binding site for the aptamer on the surface of the protein target. It includes an expert inspection of the protein structure and/or docking of short oligonucleotides to the whole surface of the protein. The docking appears to be preferable. In our case, a visual inspection has suggested that the region of the F′-G helix of cytochrome P450 51A1 (Fig. 1, site I) is a potential binding site because it is enriched with positively charged lysine and arginine residues. However, the docking study did not confirm this hypothesis; another region was selected as the potential binding site because it contains cavity with a positive potential on the protein surface.

The second step involves selection of oligonucleotides that can act as the recognition part of the aptamer. Usually, aptamers are 25–40 nucleotides long. However, only a small portion of those nucleotides interact directly with the target. The most studied aptamer, which is the thrombin-binding aptamer, is a 15-mer oligonucleotide (it has the G-quadruplex structure) that interacts with thrombin (according to the crystal structure, pdb 1HAO) through two loops containing only two nucleotides (Padmanabhan and Tulinsky, 1996). A temporary interaction of the other nucleotides of the aptamer with a protein was observed during a long simulation of the molecular dynamics (Shcherbinin and Veselovsky, 2013). Although there are a few aptamer–protein contacts, the affinity of this aptamer was high (Muller et al., 2007; Berezovski et al., 2003). For the protein–protein interactions, the major contribution to the binding energy of the complex is provided by a few amino acid residues at the protein–protein interface; these sites are called hot spots (Moreira et al., 2007; Veselovsky and Archakov, 2007). The same mechanism can be also appropriate for protein–oligonucleotide complexes. Therefore, the selection of short oligonucleotides capable of interacting with a target protein can be the starting point for the rational aptamers design. The good correlation between the calculated binding energy for the short oligonucleotides and the experimental dissociation constant for the aptamers (Fig. 4) demonstrates the efficiency of this approach.

The third step involves selecting the structural fragment of the aptamer, the main function of which is to maintain the optimal conformation of the recognition part of the aptamer. The structures of the known aptamers are quite different and include G-quadruplexes, hairpins, tetraloops, and pseudoknots (Baldrich and Zourob, 2010). In our case, a double helix was selected due to the U-like conformation of the trinucleotides in the binding site. The fusion of the recognition and structural parts generated aptamers with a hairpin structure.

The correlation between the calculated binding energy and the experimental K_d values (Fig. 5) indicates that the designed aptamers interact with the binding site selected during the first step. This behavior is confirmed by the influence of the central guanidine of the recognition part on the binding affinity. Analysis of the docking results shows that region II is most frequently associated with guanidine (Table 1); replacing this nucleotide dramatically increased the dissociation constant of the protein–aptamer complex (Table 2).

Experimental testing of seven 15-nucleotides aptamer showed that all of them could bind to cytochrome P450, however molecular dynamics and MM–PBSA results indicated that one trinucleotides (ACA) couldn't bind to the target protein and form the stable complex. The reason of the ability of hairpin-like aptamer with this trinucleotide as recognizable part to interact with the target protein might be explained by the fixed recognition part (ACA) in the optimal conformation or by the contribution of the structural part in aptamer–protein interaction.

The designed aptamers have a moderate affinity for cytochrome P450 51A1 ($K_d \sim 10^{-6}$–10^{-7} M). However, these values are similar to those of previously reported aptamers (Ahmad et al., 2011). A further optimization of their structure, including increasing their length, can enhance their affinity. The affinity and selectivity can be increased by designing bivalent aptameric constructs containing an aptamer pair that interacts with different regions on the target. Binding this type of aptamer considerably increased the aptamer affinity (Rakhmetova et al., 2011). Docking oligonucleotides on the cytochrome P450 51A1 surface revealed two additional potential binding sites for aptamers that can participate in interaction of a similar construct.

The estimated selectivity of the designed aptamers showed that these aptamers are unable to interact with other components of

Please cite this article in press as: Shcherbinin, D.S., et al. Computer-aided design of aptamers for cytochrome p450. J. Struct. Biol. (2015), http://dx.doi.org/10.1016/j.jsb.2015.07.003

microsomal monooxygenase system of cytochrome P450 (NADPH-cytochrome P450 reductase и cytochrome b_5), and with major blood proteins (serum albumin and thrombin). Nevertheless, these aptamers can bind to cytochrome P450 3A4, the member of cytochrome P450 superfamily. This superfamily is characterized by very conservative spatial structures, although its members have low amino acid sequence identity (identity between CYP51A and CYP3A4 is approximately 20%). The regions of these cytochromes P450 that form the potential aptamer binding sites also have a low identity. Nevertheless, both of them are enriched with aromatic and positively charged residues; therefore, the properties of the aptamer binding sites of these cytochrome P450 structures might be similar. Recently, for cytochrome P450 2B4 this region was identified as the binding site for cytochrome b_5 that participates in the regulation of cytochrome P450 activity and electron transport (Ahuja et al., 2013). Site-directed mutagenesis confirmed that the positively charged and aromatic residues of this region are important for cytochrome b_5 binding (Ahuja et al., 2013; Bridges et al., 1998; Chudaev et al., 2001). Although cytochromes 51A1, 3A4 and 2B4 belong to highly divergent families, they preserve the properties of this region of their structures to interact with a mutual partner. Thus it can explain why aptamers designed for cytochrome P450 51A1 can interact with cytochrome P450 3A4. Consequently, these aptamers can also interact with some other microsomal cytochromes P450. Nevertheless, optimizing the aptamer structures (using computer-based or experimental methods) or designing bivalent aptameric constructs can increase their selectivity and affinity.

Thus, we developed an *in silico* approach for aptamer design, and used it to construct aptamers for cytochrome P450. There are the first aptamers for proteins from the cytochrome P450 superfamily. The aptamers designed against CYPs can be used to modulate the protein–protein interactions in monooxygenase systems, thus changing the activity of these complex enzyme systems.

Appendix A. Supplementary data

Supplementary data associated with this article can be found, in the online version, at http://dx.doi.org/10.1016/j.jsb.2015.07.003.

References

Ahmad, K.M., Oh, S.S., Kim, S., McClellen, F.M., Xiao, Y., Soh, H.T., 2011. Probing the limits of aptamer affinity with a microfluidic SELEX platform. PLoS One 6, 27051.

Ahuja, S., Jahr, N., Im, S.C., Vivekanandan, S., Popovych, N., Le Clair, S.V., Huang, R., Soong, R., Xu, J., Yamamoto, K., Nanga, R.P., Bridges, A., Waskell, L., Ramamoorthy, A., 2013. A model of the membrane-bound cytochrome b5–cytochrome P450 complex from NMR and mutagenesis data. J. Biol. Chem. 288, 22080–22095.

Baldrich, E., Zourob, M., 2010. Aptamers: versatile tools for reagentless aptasensing. Recognit. Receptors Biosens., 675–772, Chap 17.

Balogh, Z., Lautner, G., Bardyczy, V., Komorowska, B., Gyurcsányi, R.E., Mészáros, T., 2010. Selection and versatile application of virus-specific aptamers. FASEB J. 24, 4187–4195.

Barcellos, G.B., Pauli, I., Caceres, R.A., Timmers, L.F., Dias, R., de Azevedo Jr., W.F., 2008. Molecular modeling as a tool for drug discovery. Curr. Drug Targets 9, 1084–1091.

Berezovski, M., Nutiu, R., Li, Y., Krylov, S.N., 2003. Affinity analysis of a protein–aptamer complex using nonequilibrium capillary electrophoresis of equilibrium mixtures. Anal. Chem. 75, 1382.

Bridges, A., Gruenke, L., Chang, Y.T., Vakser, I.A., Loew, G., Waskell, L., 1998. Identification of the binding site on cytochrome P450 2B4 for cytochrome b5 and cytochrome P450 reductase. J. Biol. Chem. 273, 17036-1704.

Case, D.A., Darden, T.A., Cheatham III, T.E., Simmerling, C.L., Wang, J., Duke, R.E., Luo, R., Merz, K.M., Pearlman, D.A., Crowley, M., Walker, R.C., Zhang, W., Wang, B., Hayik, S., Roitberg, A., Seabra, G., Wong, K.F., Paesani, F., Wu, X., Brozell, S., Tsui, V., Gohlke, H., Yang, L., Tan, C., Mongan, J., Hornak, V., Cui, G., Beroza, P., Mathews, D.H., Schafmeister, C., Ross, W.S., Kollman, P.A., 2006. AMBER 9. University of California, San Francisco.

Chudaev, M.V., Gilep, A.A., Usanov, S.A., 2001. Site-directed mutagenesis of cytochrome b5 for studies of its interaction with cytochrome P450. Biochemistry (Mosc.) 66, 667–681.

Chushak, Y., Stone, M.O., 2009. *In silico* selection of RNA aptamers. Nucleic Acids Res. 37, 87.

Citartan, M., Gopinath, S.C., Tominaga, J., Tan, S.C., Tang, T.H., 2012. Assays for aptamer-based platforms. Biosens. Bioelectron. 34, 1–11.

Connor, A.C., McGown, L.B., 2006. Aptamer stationary phase for protein capture in affinity capillary chromatography. J. Chromatogr. A 1111, 115–119.

Dailey, M.M., Hait, C., Holt, P.A., Maguire, J.M., Meier, J.B., Miller, M.C., Petraccone, L., Trent, J.O., 2009. Structure-based drug design: from nucleic acid to membrane protein targets. Exp. Mol. Pathol. 86, 141–150.

Davis, K.A., Lin, Y., Abrams, B., Jayasena, S.D., 1998. Staining of cell surface human CD4 with 2'-F-pyrimidine-containing RNA aptamers for flow cytometry. Nucleic Acids Res. 26, 3915–3924.

Deng, Q., German, I., Buchanan, D., Kennedy, R.T., 2001. Retention and separation of adenosine and analogues by affinity chromatography with an aptamer stationary phase. Anal. Chem. 73, 5415–5421.

Dey, B., Thukral, S., Krishnan, S., Chakrobarty, M., Gupta, S., Manghani, C., Rani, V., 2012. DNA-protein interactions: methods for detection and analysis. Mol. Cell. Biochem. 365 (1–2), 279–299.

Ferreira, C.S., Papamichael, K., Guilbault, G., Schwarzacher, T., Gariepy, J., Missailidis, S., 2008. DNA aptamers against the MUC1 tumour marker: design of aptamer-antibody sandwich ELISA for the early diagnosis of epithelial tumours. Anal. Bioanal. Chem. 390, 1039.

German, I., Buchanan, D.D., Kennedy, R.T., 1998. Aptamers as ligands in affinity probe capillary electrophoresis. Anal. Chem. 70, 4540–4545.

Gnedenko, O.V., Kaluzhskiy, L.A., Molnar, A.A., Yantsevich, A.V., Mukha, D.V., Gilep, A.A., Usanov, S.A., Stonik, V.A., Ivanov, A.S., Lisitsa, A.V., Archakov, A.I., 2013. The SPR-based biosensor test system for analysis of small compounds interaction with human cytochrome P450 51A1 (CYP51A1). Biochem. (Mosc.) Suppl. B: Biomed. Chem. 7, 187–195.

Guryev, O.L., Gilep, A.A., Usanov, S.A., Estabrook, R.W., 2001. Interaction of apo-cytochrome b5 with cytochromes P4503A4 and P45017A: relevance of heme transfer reactions. Biochemistry 40, 5018–5031.

Humphrey, W., Dalke, A., Schulten, K., 1996. VMD – Visual Molecular Dynamics. J. Mol. Graphics 14, 33–38.

Ivanov, A.S., Gnedenko, O.V., Molnar, A.A., Archakov, A.I., Podust, L.M., 2010. FMN binding site of yeast NADPH-cytochrome P450 reductase exposed at the surface is highly specific. ACS Chem. Biol. 20, 767–776.

Joseph-McCarthy, D., Campbell, A.J., Kern, G., Moustakas, D., 2014. Fragment-based lead discovery and design. J. Chem. Inf. Model. 54 (3), 693–704.

Kanwar, J.R., Roy, K., Kanwar, R.K., 2011. Chimeric aptamers in cancer cell-targeted drug delivery. Crit. Rev. Biochem. Mol. Biol. 46, 459–477.

Keefe, A.D., Schaub, R.G., 2008. Aptamers as candidate therapeutics for cardiovascular indications. Curr. Opin. Pharmacol. 8, 147–152.

Kumar, A., Voet, A., Zhang, K.Y., 2012. Fragment based drug design: from experimental to computational approaches. Curr. Med. Chem. 9 (30), 5128–5147.

Lang, P.T., Brozell, S.R., Mukherjee, S., Pettersen, E.F., Meng, E.C., Thomas, V., Rizzo, R.C., Case, D.A., James, T.L., Kuntz, I.D., 2009. DOCK 6: combining techniques to model RNA-small molecule complexes. RNA 15, 1219–1230.

Lepesheva, G.I., Waterman, M.R., 2004. CYP51 – the omnipotent P450. Mol. Cell. Endocrinol. 215, 165–170.

Ma, B., Wolfson, H.J., Nussinov, R., 2001. Protein functional epitopes: hot spots, dynamics and combinatorial libraries. Curr. Opin. Struct. Biol. 11, 364–369.

Ma, D.L., Chan, D.S., Lee, P., Kwan, M.H., Leung, C.H., 2011. Molecular modeling of drug-DNA interactions: virtual screening to structure-based design. Biochimie 93, 1252–1266.

Mayer, G., 2009. The chemical biology of aptamers. Angew Chem. Int. Ed. Eng. 48, 2672–2689.

Moreira, I.S., Fernandes, P.A., Ramos, M.J., 2007. Hot spots – a review of the protein–protein interface determinant amino-acid residues. Proteins 68, 803–812.

Mukha, D.V., Feranchuk, S.I., Gilep, A.A., Usanov, S.A., 2011. Molecular modeling of human lanosterol 14α-demethylase complexes with substrates and their derivatives. Biochemistry (Mosc.) 76, 175–185.

Muller, J., Wulffen, B., Potzch, B., Mayer, G., 2007. Multidomain targeting generates a high-affinity thrombin-inhibiting bivalent aptamer. ChemBioChem 8, 2223–2226.

Ng, E.W., Shima, D.T., Calias, P., Cunningham Jr., E.T., Guyer, D.R., Adamis, A.P., Pegaptanib, 2006. A targeted anti-VEGF aptamer for ocular vascular disease. Nat. Rev. Drug Discov. 52, 123–132.

Ni, X., Castanares, M., Mukherjee, A., Lupold, S.E., 2011. Nucleic acid aptamers: clinical applications and promising new horizons. Curr. Med. Chem. 18, 4206–4214.

Padmanabhan, K., Tulinsky, A., 1996. An ambiguous structure of a DNA 15-mer thrombin complex. Acta Crystallogr. 52, 272–282.

Rakhmetova, S.Yu., Radko, S.P., Gnedenko, O.V., Bodoev, N.V., Ivanov, A.S., Archakov, A.I., 2011. Comparative thermodynamic analysis of thrombin interaction with anti-thrombin aptamers and their heterodimeric construct. Biochem. (Mosc.) Suppl. B: Biomed. Chem. 5, 139–143.

Sa-Debeljak, N., Fink, M., Rozman, D., 2003. Many facets of mammalian lanosterol 14a-demethylase from the evolutionarily conserved cytochrome P450 family CYP51. Arch. Biochem. Biophys. 409, 159–171.

Sanchez, I.E., Ferreiro, D.U., Dellarole, M., de Prat-Gay, G., 2010. Experimental snapshots of a protein–DNA binding landscape. PNAS 107, 7751–7756.

Sefah, K., Shangguan, D., Xiong, X., O'Donoghue, M.B., Tan, W., 2010. Development of DNA aptamers using Cell-SELEX. Nat. Protoc. 5, 1169–1185.

Please cite this article in press as: Shcherbinin, D.S., et al. Computer-aided design of aptamers for cytochrome p450. J. Struct. Biol. (2015), http://dx.doi.org/10.1016/j.jsb.2015.07.003

Shcherbinin, D.S., Veselovsky, A.V., 2013. Investigation of interaction of thrombin-binding aptamer with thrombin and prethrombin-2 by simulation of molecular dynamics. Biophysics 58, 315–323.

Stoltenburg, R., Reinemann, C., Strehlitz, B., 2007. SELEX – a (r)evolutionary method to generate high-affinity nucleic acid ligands. Biomol. Eng. 24, 381–403.

Strushkevich, N., Usanov, S.A., Park, H.W., 2010. Structural basis of human CYP51 inhibition by antifungal azoles. J. Mol. Biol. 397, 1067–1078.

Tombelli, S., Minunni, M., Luzi, E., Mascini, M., 2005. Aptamer-based biosensors for the detection of HIV-1 Tat protein. Bioelectrochemistry 67, 135–141.

Ulrich, H., Trujillo, C.A., Nery, A.A., Alves, J.M., Majumder, P., Resende, R.R., Martins, A.H., 2006. DNA and RNA aptamers: from tools for basic research towards therapeutic applications. Comb. Chem. High Throughput Screen. 9, 619–632.

Veselovsky, A.V., Archakov, A.I., 2007. Inhibitors of Protein-Protein Interactions as Potential Drugs. Curr. Comput. Aided Drug Des. 3, 51–58.

Waterman, M.R., Lepesheva, G.I., 2005. Sterol 14 alpha-demethylase, an abundant and essential mixed-function oxidase. Biochem. Biophys. Res. Commun. 338, 418–422.

Please cite this article in press as: Shcherbinin, D.S., et al. Computer-aided design of aptamers for cytochrome p450. J. Struct. Biol. (2015), http://dx.doi.org/10.1016/j.jsb.2015.07.003